HIGH RESOLUTION CHANNEL ESTIMATION USING THE EXPECTATION MAXIMIZATION ALGORITHMS

Omar Qaise, LSE Space Engineering & Operations AG, Germany
Stephan Sand, German Aerospace Center (DLR), Germany
Prof. Martin Schneider, Bremen University, Germany

Email: omar.qaise@lsespace.com, stephan.sand@dlr.de,
martin.schneider@hf.uni-bremen.de

Abstract

One of the most important tasks of satellite navigation systems consists of propagation delay estimation and timing tracking. Related problems appear when considering wideband code division multiple access (WCDMA) systems used in mobile communication when transmitted spread spectrum signals propagate along reflected paths, especially in urban areas with high buildings. These spreading sequences have an inherent resistance against interference errors. Contrary to mobile radio systems, even sub-chip synchronization accuracy is required for navigation systems to estimate the position and velocity accurately. The reason for this multipath sub-chip resolution is the connection between propagation delay errors and delay locked loop (DLL) tracking: The multipath propagation leads to a bias of the loop resulting in a positioning error even in the noiseless case. In order to mitigate this multipath effect, a maximum likelihood (ML) estimator is formulated taking into account the reflected signals. However, having several amplitudes and delays as parameters, the resulting system of equations does no longer suggest a straightforward exact solution without dramatic increase in complexity. The potential of the Expectation Maximization (EM) algorithm lies in the fact that it iteratively approximates the ML and significantly reduces the complexity by breaking down the multi-dimensional non-linear optimization problem of the ML into a number of one dimensional ones. This paper investigates the performance of the EM algorithm, and its companion Space Alternating Generalized EM (SAGE) algorithm, for high resolution channel estimation of Global Navigation Satellite System (GNSS) signals, e.g., the Global Positioning System (GPS) and the Galileo navigation system. Also, the efficiency of these algorithms is compared to the wide and narrow correlators, which are currently employed in GNSS receivers to mitigate the multipath effect. The EM methods successfully estimate parameters of impinging waves for navigation systems due to their good performance, fast convergence, and low complexity. Furthermore, a novel extension to the EM/SAGE algorithms is introduced, by combining their attractive features with the signal-matched and code-matched correlator techniques used in complexity reduction.

1. INTRODUCTION

Position estimation in global navigation satellite systems (GNSSs) like the GALILEO system is typically performed using pseudorange measurements between several satellites and the receiver. A precise location determination requires the synchronization of the respective line of sight (LOS) path between the transmitters and the receivers with sub chip accuracy. Due to multipath effect, the reception of signal replicas results in biased pseudoranges that will deteriorate the position estimation. Hence, it is necessary to mitigate the multipath effects in an efficient way. In a mass market receiver, this may be partially achieved by a narrow early minus late (NEML) or other correlators. Alternative to the correlator approach, maximum likelihood (ML) based multipath estimation nearly mitigates all adverse multipath effects on the pseudoranges [1]. A suboptimum multipath estimation based on the iterative expectation maximization (EM) algorithm [2] or the improved space alternating generalized expectation maximization (SAGE) algorithm [3] has been investigated by [4]. J. Selva developed in [5], [6], [7] the framework for complexity reduced maximum likelihood (ML) channel estimation (CE) methods in navigation receivers which allows an efficient implementation. This framework comprised different subspace approaches which consisted of code or signal matched filter (MF) banks or principal components (PCs) filter or a suitable combination of these two algorithms.

In this paper we investigate the complexity reduction preprocessing of the navigation signals before applying the EM or SAGE algorithms. The performance will be assessed and compared to the classical EM/SAGE algorithms with no preprocessing.

Notation: vectors (e.g. $\mathbf{y} \in \mathbf{C}^N$) and matrices are denoted by small and capital bold letters. 'E[$\bullet$]', '$\hat{\bullet}$', 'T', '$*$', and 'H' denote the expectation, estimation, transposed, complex conjugate, and Hermitian operators. The operator '$\otimes$' expresses the calculation of the Kronecker product between two matrices. If applied to a vector $\mathbf{x} \in \mathbf{C}^N$, the

operator diag $\{x\} \in \mathbf{C}^{N\times N}$ denotes the matrix with the elements of $x \in \mathbf{X}^N$ on its diagonal. y := FFT$\{x\}$ $\in \mathbf{C}^N$ represents the fast Fourier transform (FFT) of a vector $x \in C^N$ whose dimension N is a power of 2. The i-th column of the unit matrix $1_N \in \mathbf{C}^{N\times N}$ is termed $e_i^{(N)}$. $0_N \in \mathbf{C}^N$ represents the N-dimensional column vector with zero elements.

2. CHANNEL MODEL

In order to demonstrate the influence of the multipath propagation on the estimation performance of the LOS path and thereby on the position estimation of the MS, the channel is modeled as a fixed channel of length L

$$h(\tau,t) = h(\tau) := \sum_{l=0}^{L-1} a_l \delta(\tau - \tau_l) \tag{1}$$

where the number of channel coefficients L is assumed to be known to the receiver. The results in this paper can be considered as a worst case bound compared to the typically considered Rayleigh fading channel model, because multipath propagation undergoing Rayleigh fading always causes smaller positioning errors than fixed multipath propagation does.

3. INTERPOLATION MODEL

As a pulse shape for the transmission considered in this paper, we make use of root raised cosine (RRC) pulses $g(t)$ which are defined by an one sided limit frequency f_N and a roll off factor β. We may write the direct sequence spread spectrum (DS-SS) transmit (Tx) signal as

$$\begin{aligned} s(t) := &\sum_{m=0}^{M-1} d_{p,m} \sum_{n=o}^{N-1} c_{p,n}\, g(t - mT - nT_c) + \\ &\sum_{m=0}^{M-1} d_{D,m} \sum_{n=0}^{N-1} c_{D,n}\, g(t - mT - nT_c) \end{aligned} \tag{2}$$

where T and $T_c = 1/R_c$ denote the frame duration and chip duration with R_c being the chip rate. The pilot and data symbol sequences $d_{P,m}$ and $d_{D,m}$, $m = 0, \ldots, M-1$ are taken from quadrature phase shift keying (QPSK) modulation. M codewords form the considered time interval for CE. The spreading code sequences $c_{p,n}$, $n = 0, \ldots, N-1$ for the pilots and $c_{D,n}$, $n = 0, \ldots, N-1$ for the data are orthogonal Gold codes of length N in this contribution. In order to obtain a suitable matrix vector factorization beginning from (2), we choose the sampling frequency f_S as integer multiple of the chip rate R_C yielding $Q := f_S / R_C$ samples per chip. If we assume an observation interval of duration MNT_C, we can define M successive signal vectors $s_{mn} \in C^{NQ}$, $m = 0, \ldots, M$ as $s_m := [s[(m-1)NQ], \ldots, s[mNQ-1]]^T$, with $s[k] := s(k/f_s)$, $k = (m-1)NQ, \ldots, mNQ-1$. Therefore, the sampled Tx signal in matrix vector notation in (2) is $s = [s_1^T, \ldots, s_M^T]^T \in C^{MNQ}$, and $s_m = d_{P,m}\mathbf{C}_P g + d_{D,m}\mathbf{C}_D g$, $m = 1, \ldots, M$. $\mathbf{C}_P, \mathbf{C}_D \in C^{NQ\times N_{pp}}$ are the pilot and data code matrices, and $g \in C^{N_{pp}}$ is the zero padded sampled RRC pulse. N_{pp} is chosen as the next power of two exceeding or equal to the number of pulse samples N_p, for the FFT based pulse interpolation. Therefore, $g \in C^{N_{pp}}$ contains the N_p samples of the RRC pulse padded two times with $N_Z = (N_{PP} - N_P)/2$ zeros, i. e., $\mathbf{g} = [0_{N_z}^T, g(-(N_P-1)/2), \ldots, g((N_P-1)/2), 0_{N_z}^T]^T \in C^{N_{pp}}$.

The pulse interpolation technique enables the following pulse shifting [6]

$$g(\tau) \approx \mathbf{F}^{-1}\mathrm{diag}\{\mathrm{FFT}\{g\}\}\phi(\tau) \tag{3}$$

The columns of $\mathbf{C}_P \in C^{NQ\times N_{pp}}$ and $\mathbf{C}_D \in C^{NQ\times N_{pp}}$ are circularly shifted versions of $c_p \otimes e_1^{(Q)} \in \mathbf{C}^{NQ}$ and $c_D \otimes e_1^{(Q)} \in \mathbf{C}^{NQ}$. The matrix $\mathbf{F}^{-1} \in \mathbf{C}^{N_{pp}\times N_{pp}}$ is the permuted inverse Fourier matrix $(\mathbf{F}^{-1})_{k,\ell} = \exp(j(2\pi/N_{PP})(k - N_{PP}/2)(\ell - N_{PP}/2))$, $k, \ell = 1, \ldots, N_{PP}$. $\Phi(\tau) \in C^{N_{pp}}$ is a Vandermond vector, i. e., $(\Phi(\tau))_k = \exp(-j(2\pi Q/N_{PP})(k - N_{PP}/2)\tau)$, $k = 1, \ldots, N_{PP}$. Having determined the pulse interpolation in (3), we can now formulate the interpolation representation of the spreading signal using the pilot and data code matrices $\mathbf{C}_P, \mathbf{C}_D \in C^{NQ\times N_{pp}}$ as $s(\tau) = [s_1^T(\tau), \ldots, s_M^T(\tau)]^T \in C^{MNQ}$, where $s_m(\tau) = d_{P,m}\mathbf{C}_P g(\tau) + d_{D,m}\mathbf{C}_D g(\tau) = d_{P,m}\, s_P(\tau) + d_{D,m}\, s_D(\tau)$ for $m = 1, \ldots, M$. The abbreviations $\mathbf{C}_P g(\tau) = s_P(\tau)$ and $\mathbf{C}_D g(\tau) = s_D(\tau)$ represent the interpolated pilot and data signal.

At this point it is convenient to derive a second interpolation representation for the pilot and data code $\mathbf{C}_P$, $\mathbf{C}_D \in C^N$. The code interpolation bases on the same interpolation method as (3). Again, the two distinct parameters are f_N as band limiting frequency f_S as sampling frequency of the RRC pulse. A Dirac delta function $\delta(t)$ which is transformed into the frequency domain, bandlimited to f_N, and transformed back into time domain yields the sinc function $\mathrm{sinc}(t) = \sin(2\pi f_N t)/(\pi t)$. We proceed now in the same way as before with the interpolation of the RRC pulse: $\delta \in C^{N_{pp}}$ contains the N_P samples of the sinc function padded two times with $N_Z = (N_{PP} - N_P)/2$ zeros to reach N_{PP}; $\delta = [0_{N_z}^T, \delta(-(N_P-1)/2), \ldots, \delta((N_P-1)/2), 0_{N_z}^T]^T \in C^{N_{pp}}$. The corresponding interpolation representation to (3) is then

$$\delta(\tau) \approx \mathbf{F}^{-1}\mathrm{diag}\{\mathrm{FFT}\{\delta\}\}\phi(\tau) \tag{4}$$

We have as interpolated pilot code $c_P(\tau) = \mathbf{C}_P\, \delta(\tau)$ and $c_D(\tau) = \mathbf{C}_D\, \delta(\tau)$ as interpolated data code.

4. TRANSMISSION MODEL

After transmission over the channel, the received signal (Rx) vector becomes

(5) $$y := \sum_{l=1}^{L} a_l s(\tau_l) + n = S(\tau) + n \in \mathbf{C}^{MNQ}$$

where $n(t)$ describes the zero-mean additive white Gaussian noise (AWGN) of the power $\sigma^2 = E[n(t)^2]$, and $\mathbf{S}(\tau) = [s(\tau_1), \ldots, s(\tau_L)] \in C^{MNQ \times L}$ and $\mathbf{a} = [a_1, \ldots, a_L]^T \in C^L$ form the signal matrix and amplitude vector.
M successive observation vectors $y_m \in C^{NQ}$ $(m = 1, \ldots, M)$ form the whole observation vector $y_m = [y_1^T(\tau), \ldots, y_M^T(\tau)]^T \in C^{MNQ}$, therefore the m-observation vector in (5) is: $y_m = \sum a_l s_m + n_m \in C^{NQ}$

Similar, we can write the noise vector as $n = [n_1^T, \ldots, n_M^T]^T \in C^{MNQ}$, $n_m = [n((m-1)NQ/f_S), \ldots, n((mNQ-1)/f_S)]^T \in C^{NQ}$, $m = 1, \ldots, M$.

5. ML CHANNEL ESTIMATION IN REDUCED DIMENSION

For $y_m \in C^{MNQ}$, the ML estimate $\{\hat{a}, \hat{\tau}\} \in \mathbf{C}^L$ is found according to $\{\hat{a}, \hat{\tau}\} = \arg\min_{\{a,\tau\}} \|y - S(\tau)a\|^2$. The EM/SAGE algorithms can be used to find the ML estimate. However this might be a complex operation, specially with a large number of samples and fast computation requirement in navigation systems. To decrease computational complexity, we propose to use the following two stage complexity reduction before computing the ML estimates.

5.1. Code/Signal Matched Correlators and Principal Component Analysis

As a first step, the pilot symbols in the sampled Rx vector y are demodulated and filtered codeword by codeword by an orthonormalized correlatorbank of N_{CC} pilot code matched correlators (CMCs) $Q_{cc} \in C^{NQ \times N_{CC}}$.

This matrix is obtained from a QR decomposition of $\mathbf{C}_{CC} = [c_P(\tau_G,1), \ldots, c_P(\tau_G, N_{CC})] = \mathbf{Q}_{cc}\mathbf{R}_{cc}$ yielding the output of the correlatorbank as

(6) $$y_{CC} := \sum_{m=1}^{M} d_{P,m} Q_{CC}^H y_m = \sum_{m=1}^{M} d_{P,m} Q_{CC}^H \left(\sum_{l=1}^{L} s_m(\tau_l) + n_m\right)$$
$$= MQ_{CC}^H \sum_{l=1}^{L} s_P(\tau_l) + \sum_{m=1}^{M} d_{P,m} Q_{CC}^H n_m \in C^{N_{CC}}$$

where we have exploited the orthogonality between the pilot CMC matrix $Q_{cc} \in C^{NQ \times N_{CC}}$ and the data code matrix $\mathbf{C}_D \in C^{NQ \times N_{CC}}$. $\tau_G = [\tau_{G,1}, \ldots, \tau_{G,Ncc}]$ defines the N_{CC} node values for the CMCs. In the following further complexity reduction using principal components (PCs), the introduction of the filtered pilot signals $s_{p,cc} = Q_{CC}^H s_p(\tau) \in C^{N_{CC}}$ is helpful. We calculate the autocorrelation $R_{s_p} = E[s_p(\tau) s_p(\tau)^H] \in C^{NQ \times NQ}$ and

$$R_{s_{p,CC}} = E[s_{p,cc}(\tau) s_{p,cc}(\tau)^H] = Q_{CC}{}^H R_{s_p} Q_{CC} \in C^{N_{CC} \times N_{CC}}$$

exploiting *a-priori* information of the channel taps. Here we choose a robust a-priori assumption that is a robust distribution in $[-2T_C, 2T_C]$ [6, 7]

(7) $$R_{s_p} = E[s_p(\tau) s_p(\tau)^H] = \int_{-2T_C}^{2T_C} s_p(\tau) s_p(\tau)^H \frac{1}{4T_C} d\tau$$

For the second stage of complexity reduction, it is necessary to calculate the eigenvalue decomposition (EVD) of $R_{s_p} = Q\Lambda Q^H$. $Q = [q_1, \ldots, q_{Ncc}] \in C^{N_{CC} \times N_{CC}}$ contains in its columns the respective eigenvectors and $\Lambda = \text{diag}\{[\lambda_1, \ldots, \lambda_{Ncc}]\} \in C^{N_{CC} \times N_{CC}}$ is the diagonal matrix containing the eigenvalues in descending order, i.e. $\lambda_1 > \ldots > \lambda_{Ncc} > 0$. For a given number $N_{PC} \le N_{CC}$ of PCs, the autocorrelation matrix is approximated by $R_{s_{p,CC}} \approx \sum_{k=1}^{N_{PC}} \lambda_k q_k q_k{}^H$. As a result we have

(8) $$y_{PC} := Q_{PC}^H y_{CC} \in C^{N_{PC}}$$

where $Q_{PC} = [q_1, \ldots, q_{Npc}] \in C^{N_{CC} \times N_{PC}}$ is the PC eigenspace matrix. At this place it is also convenient to define the two fold filtered pilot signal $s_{p,pc}(\tau) = Q_{PC}^H Q_{CC}^H s_p(\tau) \in C^{N_{PC}}$ which we will need in the following subsections. We can now determine the ML estimate of y_{PC} and $s_{P,PC}(\tau)a \in C^{N_{PC}}$ ($s_{P,PC}(\tau) = [s_{P,PC}(\tau_1), \ldots, s_{P,PC}(\tau_L)] \in C^{N_{PC} \times L}$) instead of $y \in C^{MNQ}$ and $\mathbf{S}(\tau)\mathbf{a} \in C^{MNQ}$ to reduce complexity.

This approach was implemented based on the code matched correlator (CMC) using code samples [+1,-1] of $\mathbf{C}_{CC} = [c_P(\tau_G,1), \ldots, c_P(\tau_G, N_{CC})]$, $c_P(\tau) = \mathbf{C}_P\, \delta(\tau)$. If we apply the same approach using bandlimited RRC pulse signals $g \in C^{N_{pp}}$ we get what we call a signal matched correlator (SMC).

5.2. Expectation Maximization Algorithm

Alg. 1 sums up the different steps belonging to the EM algorithm. All pairs of channel parameters $\{\tau_\ell, a_\ell\}$, $\ell = 1, \ldots, L$ are estimated in parallel beginning with some initial estimates $\hat{\tau}^{(0)} = [\hat{\tau}_1^{(0)}, \ldots, \hat{\tau}_L^{(0)}] \in C^L$ and $\hat{a}^{(0)} = [\hat{a}_1^{(0)}, \ldots, \hat{a}_L^{(0)}] \in C^L$ for the channel taps and amplitudes.
We observe the typical structure with the expectation (E) step (line 5) followed by the maximization (M) step (lines 8 to 9). The iterative parallel estimation of $\{\tau_\ell, a_\ell\}$, $\ell = 1, \ldots, L$ is repeated until a required estimation accuracy is achieved or the maximum number of iterations $N_{itermax}$ is exceeded.

Alg. 1 Computation Steps for the EM Algorithm

1: Input: observation vector $y_{\text{PC}} \in \mathbb{C}^{N_{\text{PC}}}$, maximum number of iterations N_{itermax}, estimation accuracy TOL,
2: initial estimations $\{\hat{\boldsymbol{\tau}}^{(0)} \in \mathbb{C}^L, \hat{\boldsymbol{a}}^{(0)} \in \mathbb{C}^L\}$, coefficients $\beta_\ell,\ \ell = 1, \ldots, L$, iterations counter $k = 0$
3: **repeat**
4: **for** $\ell = 1, \ldots, L$ **do**
5: $\hat{\boldsymbol{x}}_\ell^{(k)} = (1 - \beta_\ell)\hat{a}_\ell^{(k)} s_{\text{P,PC}}(\hat{\tau}_\ell^{(k)}) + \beta_\ell(y_{\text{PC}} - \sum_{\ell'=1,\ell'\neq\ell}^{L} \hat{a}_{\ell'}^{(k)} s_{\text{P,PC}}(\hat{\tau}_{\ell'}^{(k)})) \in \mathbb{C}^{N_{\text{PC}}}$
6: **end for**
7: **for** $\ell = 1, \ldots, L$ **do**
8: $\hat{\tau}_\ell^{(k+1)} = \underset{\tau_\ell}{\operatorname{argmax}}\{|s_{\text{P,PC}}(\tau_\ell)^{\text{H}} \hat{\boldsymbol{x}}_\ell^{(k)}|^2\}$
9: $\hat{a}_\ell^{(k+1)} = s_{\text{P,PC}}(\hat{\tau}_\ell^{(k+1)})^{\text{H}} \hat{\boldsymbol{x}}_\ell^{(k)} / \|s_{\text{P,PC}}(\hat{\tau}_\ell^{(k+1)})\|_2^2$
10: **end for**
11: $k \rightarrow k + 1$
12: **until** $\|\hat{\boldsymbol{\tau}}^{(k)} - \boldsymbol{\tau}\|_2^2 + \|\hat{\boldsymbol{a}}^{(k)} - \boldsymbol{a}\|_2^2 < \text{TOL}$ or $k > N_{\text{itermax}}$

5.3. Space Alternating Generalized Expectation Maximization Algorithm

Alg. 2 shows the successive steps belonging to the SAGE algorithm. Contrary to the EM algorithm, all pairs of channel parameters are estimated sequentially, and again, we can observe in line 5 the E step and in line 6 and 7 the M step. This iterative estimation is repeated at most N_{itermax} times or is stopped earlier if a required accuracy for channel estimation is already reached.

Alg. 2 Computation Steps for the SAGE Algorithm

1: Input: observation vector $y_{\text{PC}} \in \mathbb{C}^{N_{\text{PC}}}$, maximum number of iterations N_{itermax}, estimation accuracy TOL,
2: initial estimations $\{\hat{\boldsymbol{\tau}}^{(0)} \in \mathbb{C}^L, \hat{\boldsymbol{a}}^{(0)} \in \mathbb{C}^L\}$, iterations counter $k = 0$
3: **repeat**
4: **for** $\ell = 1, \ldots, L$ **do**
5: $\hat{\boldsymbol{x}}_\ell^{(k)} = y_{\text{PC}} - \sum_{\ell'=1}^{\ell-1} \hat{a}_{\ell'}^{(k+1)} s_{\text{P,PC}}(\hat{\tau}_{\ell'}^{(k+1)}) - \sum_{\ell'=\ell+1}^{L} \hat{a}_{\ell'}^{(k)} s_{\text{P,PC}}(\hat{\tau}_{\ell'}^{(k)}) \in \mathbb{C}^{N_{\text{PC}}}$
6: $\hat{\tau}_\ell^{(k+1)} = \underset{\tau_\ell}{\operatorname{argmax}}\{|s_{\text{P,PC}}(\tau_\ell)^{\text{H}} \hat{\boldsymbol{x}}_\ell^{(k)}|^2\}$
7: $\hat{a}_\ell^{(k+1)} = s_{\text{P,PC}}(\hat{\tau}_\ell^{(k+1)})^{\text{H}} \hat{\boldsymbol{x}}_\ell^{(k)} / \|s_{\text{P,PC}}(\hat{\tau}_\ell^{(k+1)})\|_2^2$
8: **end for**
9: $k \rightarrow k + 1$
10: **until** $\|\hat{\boldsymbol{\tau}}^{(k)} - \boldsymbol{\tau}\|_2^2 + \|\hat{\boldsymbol{a}}^{(k)} - \boldsymbol{a}\|_2^2 < \text{TOL}$ or $k > N_{\text{itermax}}$

6. SIMULATIONS

The algorithm with its three forms: Waveform Based EM/SAGE (Normal algorithm with no complexity reduction), SMC Based EM/SAGE (signal preprocessed by SMCs bank), and CMC Based EM/SAGE (signals preprocessed by CMC bank) were applied to both GPS and Galileo signals scenarios. In all simulations, the multipath channel examined is a statistical channel with only two paths: a direct signal and an indirect signal. The signals are real, there is no Doppler shift, and the indirect signal is considered to be in-phase with the direct signal, because in this case the multipath has a clear effect on the signal due to constructive interference. The same also applies to the out-of-phase multipath, but the main focus will be on the in-phase multipaths, unless otherwise specified. The static scenario is more severe to navigation signals than the mobile one. The reason is that a specific multipath always exists, and there is high possibility that the receiver solution converges after sometime to this wrong path. Contrast to that, most multipaths in mobile channels change and fade frequently (diversity). The signal scenario for subsequent multipath performance analysis is defined in TAB 1. For this scenario, the conventional receiver employs a 16.368 MHz loop bandwidth. A gold PRN code signal of 1 MHz bandwidth is used. Note that the indirect path amplitude is half as much as that of the direct signal, expressed by the Signal-to-Multipath Ratio (SMR). It is necessary to carry out an averaging over 200 code words (smoothing) to get rid of the high noise effect. This represents a gain of about 23 dB, but has the drawback of the receiver being delayed (about 0.2 s) before processing the signals.

Freq. band	L1
Center Freq.	1575.42 MHz
Mod. Scheme	BPSK(1) (C/A Code)
Chip Rate	1.023 MHz
Codeword Length	1023 Chips
Sig. Bandwidth	4 MHz
Sampling Freq.	4.092 MHz
SNR	-20 dB
SMR	3 dB
Smoothing	200 Codewords (0.2 sec)
Corr. Period	1 Codeword
Bandlimiteing Filter	FIR Hamming Window Filter

TAB 1. GPS scenario parameters

In order to assess the performance of the EM algorithm, the results will be compared to the conventional wide and narrow correlators used in satellite navigation receivers. The multipath error envelopes of the EM methods were obtained and compared to the narrow correlator performance as depicted in FIG 1. Each envelope represents the estimation bias averaged over 100 experiments, except for the narrow correlator, where it is noise free simulation. The error envelope is composed of a positive (solid) and negative (dashed) half belonging to the in-phase and out-of-phase multipaths respectively. The dark cyan curve, which represents the narrow correlator performance. The conventional Waveform Based EM error envelope has a peak error of about 21 meters at a relative multipath delay of 0.25 T_c for the in-phase part, and similarly a peak error of 23.5 meters at a delay of 0.1 T_c for the out-of-phase part. This is about 10 meters improvement over the narrow correlator peak error. After a relative delay of 0.4 T_c, the estimation bias levels off and becomes limited around 3 meters. The green error envelope of the CMC Based EM shows much better performance, bringing the maximum pseudorange error down by about 3 meters less than its Waveform Based EM companion. For multipath delays longer than 0.4 T_c, the two methods behave almost the same. In the contrary to all that, the SMC Based EM envelope shows a higher pseudorange error than all the previous methods, including the narrow correlator. The positive part has approximately the same maximum error as the narrow correlator, but the negative curve shows drastic bias to a maximum error of 55 meters at a multi path delay of half a chip period. Also note that the error peak is offset to the right compared to the other methods error peaks.

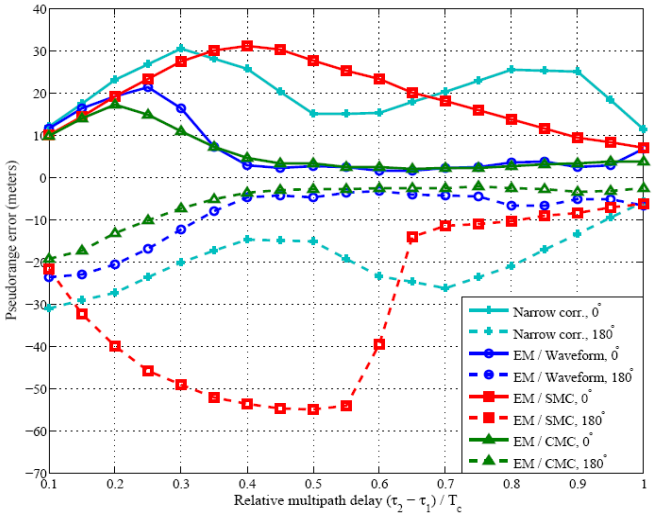

FIG 1. Multipath error envelopes of the various EM estimations applied to GPS signals.

This is due to the fact that the signal waveform involved in each method is different, being a rectangular chip sequence in the Waveform Based EM, a bell shaped correlation function for the SMC Based EM, and something in between for the CMC Based EM. The ability of the EM algorithm to distinguish between the two signals slowly vanishes towards shorter relative delays. Simulation results have shown that towards shorter relative delays of reflection, the EM algorithm more and more often converges to either two equal delay estimates ($\hat{\tau}_1 = \hat{\tau}_2$) or to the true Line-Of-Sight Signal (LOSS) delay estimate and a noisy estimate of the multipath delay, which mostly has a large difference to the true value. Thus, the performance of the EM slowly tends to the case where only the LOSS is present.
The error envelope for the wide correlator was not shown in the comparison, because it has an error many orders of magnitude higher than that of the EM algorithm and narrow correlator.

Freq. band	L1
Center Freq.	1575.42 MHz
Mod. Scheme	BOC(1,1) (E1-C signal)
Chip Rate	1.023 MHz
Codeword Length	4092 Chips
Sig. Bandwidth	10 MHz
Sampling Freq.	10.23 MHz
SNR	-20 dB
SMR	3 dB
Smoothing	50 Codewords (0.2 sec)
Corr. Period	1 Codeword
Bandlimiteing Filter	FIR Hamming Window Filter

TAB 2. Galileo scenario parameters

The next step is to apply the developed SAGE approaches to the Galileo navigation signals. The E1 BOC(1,1) signal was chosen to be tested with the algorithm, because of its simplicity and similarity to the GPS C/A signal. No navigation bits are considered to be modulated in the signal, thus only the pilot channel was examined. The secondary code in the pilot channel was omitted, so the signal is composed mainly of the primary code.

The signal scenario for subsequent multipath performance analysis is defined in TAB 2. For this scenario, the conventional receiver employs a 100 MHz loop bandwidth. In order to comply with the smoothing gain implemented for the GPS signal, 50 codewords were smoothed instead of 200, because the Galileo codeword is four times longer than the GPS code (4092 chips versus 1023 chips). The BOC(1,1) modulation widens the frequency spectrum by about a double. For this reason, and also due to the limited optimization grid used in simulation (100 samples per chip) and to avoid aliasing, a lowpass filter with cutoff frequency 5 MHz was used to bandlimit the signal, and the sampling frequency was chosen to be 10 MHz.
FIG 2 shows the positive multipath error envelopes of the SAGE applied to the Galileo signals. It is very interesting to note that the Waveform and CMC Based SAGE algorithms provide a delay estimation of zero error after 0.15 T_c and 0.2 T_c multipath delays, respectively.
Of course, there is small bias after this region, but it is out of the optimization grid and very small. We should also take into account the advantage of the high sampling frequency and wide bandwidth employed. Both the solid green and blue curves start with an initial bias of 6 meters, after it was 9 meters in the EM, and then decrease abruptly. Furthermore, the SMC Based EM maximum error is reduced, from about 17.5 meters to about 13.5 meters. The corresponding solid red curve starts decreasing after its peak at 0.2 T_c, until a multipath delay of 0.55 T_c, where it reaches a zero estimation bias, and the pseudorange can be estimated accurately. All three approaches provide better performance than the EM approaches.

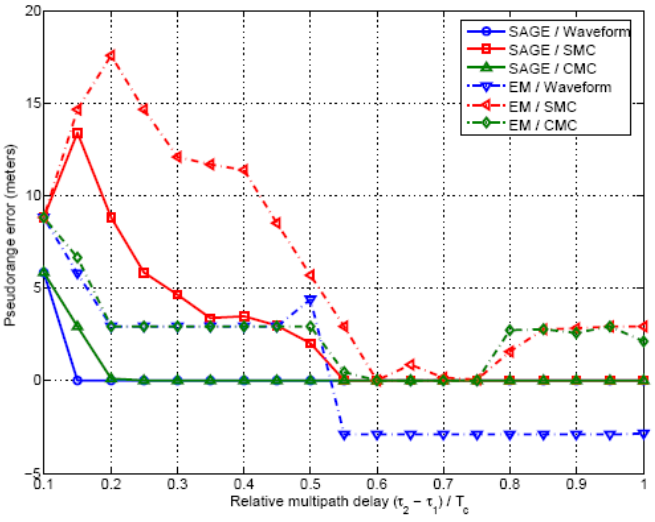

FIG 2. Positive Multipath error envelopes of the various SAGE/EM estimations applied to Galileo signals.

7. CONCLUSION

In this work, the problem of estimating the propagation time-delay of the LOSS in a GNSS receiver under the presence of severe multipath, in a static channel, was addressed. Extensions were made to these algorithms, by investigating their performance when the input signals are of low complexity but still carry the same multipath information. This has lead to the four novel approaches: SMC Based EM, CMC Based EM, SMC Based SAGE,

and CMC Based SAGE. The correlator bank prefiltering before was necessary for two reasons: on the one hand for the separation of superimposed orthogonal spreading sequences in the receiver, and on the other, a direct PC filtering would require too much computational complexity. Simulation results have shown that the bias can be reduced using the modified EM approaches compared to wide and narrow correlator methods, e.g. for GPS scenario the maximum bais improved by about 13 metres in the CMC based EM compared to the narrow correlator. The SAGE algorithms showed faster and accurate performance than the corresponding EM methods in the considered Galileo scenario. Therefore, we have designed a variant of expectation maximization (EM) and space alternating generalized expectation maximization (SAGE) based ML CE suitable especially for mass market receivers where the signal processing complexity is very critical.

8. REFERENCES

[1] M. Lentmaier and B. Krach, “Maximum Likelihood Multipath Estimation in Comparison with Conventional Delay Locked Loops*,”* in *Proceedings of ION GNSS 19th International Technical Meeting of the Satellite Division (ION 2006), Fort Worth, Texas, September 2006.*

[2] M. Feder and E. Weinstein, “Parameter Estimation of Superimposed Signals Using the EM Algorithm,” *IEEE Transactions on Acoustics, Speech, and Signal Processing, April 1988.*

[3] B. Fleury, M. Tschudin, R. Heddergott, D. Dalhaus, and K. I. Pedersen, “Channel Parameter Estimation in Mobile Radio Environments using the SAGE Algorithm,” *IEEE Journal on Selected Areas in Communications, March 1999.*

[4] F. Antreich, O. E. Rodr´ıyguez, J. A. Nossek, and W. Utschick, “Estimation of Synchronization Parameters Using SAGE in a GNSS-Receiver,” in *Proceedings of ION GNSS 18th International Technical Meeting of the Satellite Division (ION 2005), Long Beach, California, September 2005.*

[5] J. Selva, Efficient Multipath Mitigation Methods in Navigation Systems, Ph.D. thesis, Universitat Polytecnicia de Catalunya, Barcelona, Spain, 2004.

[6] J. Selva, “Complexity Reduction in the Parametric Estimation of Superimposed Signals,” *Signal Processing*, vol. 84, pp. 2325–2343, 2004.

[7] J. Selva, “An Efficient Newton-Type Method for the Computation of ML Estimators in a Uniform Linear Array,” *IEEE Transactions on Signal Processing, vol. 53, no. 6, pp. 2036–2045, 2005.*